JST: Engineering and Technology for Sustainable Development
Volume 32, Issue 3, July 2022, 042-050

Simulation Study on the Effect of Biodiesel Ratio Derived from Waste Cooking Oil on Performance and Emissions of a Single Cylinder Diesel Engine

Nguyen Tuan Nghia, Trinh Dac Phong, Nguyen Xuan Khoa*
Hanoi University of Industry, Hanoi, Vietnam
**Email: khoanx@haui.edu.vn*

Abstract

This paper presents a study on the effect of the biodiesel ratio on the performance and emissions of diesel engines. The research engine is a cylinder engine AVL-5402 that has been simulated using the software AVL-Boost.Simulated fuels include fossil diesel and biodiesel blended with the replacement rate from 0% to 50%, including B0, B10, B20, B30, B40, and B50, respectively, simulation mode at 1400 rev/min speed for maximum torque value of the engine, at the rate of 25%, 50%, and 75% load. Combustion characteristics, power, fuel consumption, and emissions are to be evaluated based on the proportions of blended biodiesel. The results show that there is a relationship between the proportion of blended biodiesel and the parameters of the engine. Specifically, as the ratio of biodiesel blend increases, peak pressure and rate of heat release decrease while peak temperature increases, the tendency to reduce engine power and increase fuel consumption increases. The emissions of CO and soot are reduced, while NOx is increased.

Keywords: Engine simulation, biodiesel, emission, mixing ratio.

1. Introduction

Due to the rapidly growing demand for fuels and petroleum products, many problems need to be solved, such as fuel depletion, environmental pollution due to engine exhaust, industrial furnaces, etc. National security is always associated with energy security, which is therefore a top priority in each country's development strategy. With the current level of oil use, the supply of oil can meet the demand for another 40–50 years if no new sources of oil are discovered. Therefore, in order to ensure long-term energy security, reduce environmental pollution and develop sustainably, many countries over the past few decades have focused on research on the use of alternative fuels with the goal of building a clean fuel industry in their country.

A number of alternative fuels such as ethanol, methanol, hydrogen, compressed natural gas (CNG), liquefied natural gas (LNG), liquefied petroleum gas (LPG), dimethyl-ether (DME), and vegetable oils have been used as alternative fuels. However, biodiesel has received considerable attention to be used as a substitute fuel for conventional petroleum.

Biofuels have been actively researched and applied by scientists as an alternative fuel. The reason is that biofuels have similar properties to fossil fuels but have the outstanding advantages of being renewable and reducing environmental pollution.

Biodiesel has already been commercialized in the transport sector and can be used in diesel engines with little or no modification [1]. Biodiesel and its blends with conventional diesel are environmentally friendly and their use in diesel engines results in reduced exhaust pollutants as compared to conventional diesel fuel [2]. Biodiesel has an attribute change over petroleum diesel fuel, which varies depending on mixing ratio and source of biodiesel. With the same type of B100 (with the same origin), when changing the blending ratio of the biodiesel mixture, the chemical properties (C:H:O ratio, surface tension, viscosity, density, etc) and the burning characteristics (low calorific value, cetane value, etc) of the biodiesel mixture also vary with different trends. The properties of biodiesel fuel directly affect the combustion and formation of pollutants, including density, calorific value, cetane value, C:H:O ratio, distillation, sulfur content. With the same volume (or mass) of fuel supplied for one cycle, the low calorific value of the fuel will directly affect the total heat supplied to the work cycle.

Some experimental investigations were conducted on diesel engines to clarify how biodiesel affects the engine's performance and exhaust emisssions [3–5]. Most of the results showed that emissions when fueled by biodiesel are reduced significantly. However, NOx emissions increase.

In addition, the value of low heat combined with the speed injection will determine the rate of heat

ISSN 2734-9381
https://doi.org/10.51316/jst.159.etsd.2022.32.3.6
Received: January 14, 2022; accepted: April 19, 2022

exerted in the cylinder. Since B100 has a lower calorific value than B0, biodiesel mixtures will also have lower calorific values than B0. The degree of thermal decomposition of B100 depends mainly on its origin. Due to the low calorific value reduction, it will reduce the maximum temperature and pressure in the cylinder when using a biodiesel blend. This will affect the economy, energy and environment of diesel engines. The self-igniting ability of diesel fuel can be determined by the cetane value. The cetane number has a decisive effect on the lag time of the fuel and therefore directly affects the temperature and pressure in the cylinder. As more oxygen is present in the chemical composition, biodiesel mixtures generally have higher experimental cations than traditional diesel [6]. This is an advantage of biodiesel when it comes to mixing and burning.

One of the problems to be studied when using biodiesel fuel is how to increase the mixing ratio in the mixture. Therefore, in this study, we will increase the mixing ratio by up to 50% and evaluate the economic and technical features of the engine.

2. Model Description

2.1. Combustion Model

The models used to develop the combustion characteristics of diesel engines are the mixture-controlled combustion (MCC) models. This model can be calculated using two processes: pre-mix combustion and controlled combustion processes.:

$$\frac{dQ_{total}}{d\alpha} = \frac{dQ_{MCC}}{d\alpha} + \frac{dQ_{PMC}}{d\alpha} \quad (1)$$

with:

Q_{total}: Total heat release over the combustion process [kJ].

Q_{PMC}: Total fuel heat input for the premixed combustion [kJ].

Q_{MCC}: Cumulative heat release for the mixture controlled combustion [kJ].

2.1.1. Ignition delay model:

The ignition delay is calculated using the Andree and Pachernegg [7] model by solving the following differential equation:

$$\frac{dI_{id}}{d\alpha} = \frac{T_{UB} - T_{ref}}{Q_{ref}} \quad (2)$$

As soon as the ignition delay integral I_{id} reaches a value of 1.0 (= at α_{id}) at the ignition delay τ_{id} is calculated from:

$$\tau_{id} = \alpha_{id} - \alpha_{SOI}$$

with:

I_{id} : ignition delay integral [-]

T_{ref}: reference temperature = 505.0 [K]

T_{UB}: unburned zone temperature [K]

Q_{ref}: reference activation energy, f(droplet, diameter, oxygen content,…) [K]

τ_{id}: ignition delay

α_{SOI}: start of injection timing [degCA]

α_{id}: ignition delay timing [degCA]

2.1.2. Mixing Controlled Combustion process:

In this regime the heat release is a function of the fuel quantity available (f_1) and the turbulent kinetic energy density (f_2):

$$\frac{dQ_{PMC}}{d\alpha} = C_{Comb}.f_1(m_F, Q_{MCC}).f_2(k, V) \quad (3)$$

with:

$f_1(m_F, Q_{MCC}) = \left(m_F - \frac{Q_{MCC}}{LVC}\right)\left(w_{Oxygen,available}\right)^{C_{EGR}}$

$f_2(k, V) = C_{Rate} \cdot \frac{\sqrt{k}}{\sqrt[3]{V}}$

C_{Comb}: combustion constant [kJ/kg/degCA]

C_{Rate}: mixing rate constant [s]

m_F: vaporized fuel mass (actual) [kg]

LVC: lower heating value[kJ/kg]

V: cylinder volume [m^3]

α: crank angle [deg CA]

$w_{Oxygen,available}$: mass fraction of available oxygen (aspirated and in EGR) at SOI [-]

C_{EGR} influent constant [-]

k: local density of turbulent kinetic energy [m^2/s^2]

$$k = \frac{E_{kin}}{m_{F,I}\left(1 + \lambda_{Diff}.m_{stoich}\right)}$$

where:

$Ekin$: kinetic jet energy [J]

$m_{F,I}$: injection fuel mass (actual) [kg]

λ_{Diff}: air Excess Ratio for diffusion burning [-]

m_{stoich}: stoichiometric mass of fresh charge [kg/kg]

2.2. Heat Transfer Model

The heat transfer to the walls of the combustion chamber, i.e., the cylinder head, the piston, and the cylinder liner, is calculated from equation [6]:

$$Q_{wi} = A_i.\alpha_w.(T_c - T_{wi}) \quad (4)$$

with:

Q_{wi} - wall heat flow

A_i – surface area

α_w - heat transfer coefficient

T_c - gas temperature in the cylinder

T_{wi} - wall temperature.

Heat transfer coefficient (α_w) is usually calculated by Woschini Model, The Woschni model published in 1978 for the high-pressure cycle is summarized as follows [9]:

$$\alpha_w = 130.D^{-0.2}.p_c^{0.8}.T_c^{-0.53}\left[C_1.c_m + C_2.\frac{V_D.T_{c,1}}{p_{c,1}.V_{c,1}}.\left(p_c - p_{c,0}\right)\right]^{0.8} \quad (5)$$

where:

C_1 = 2,28 + 0,308 .c_u/c_m

C_2 = 0,00324 for DI engines

D - cylinder bore

c_m - mean piston speed

c_u - circumferential velocity

V_D - displacement per cylinder

$p_{c,o}$ - cylinder pressure of the motored engine (bar)

$T_{c,1}$ - temperature in the cylinder at intake valve closing (IVC)

$p_{c,1}$ - pressure in the cylinder at IVC (bar)

2.3. Emission Model

2.3.1. NOx formation model

NOx formed from the oxidation reaction of nitrogen in high-temperature conditions of combustion. 6 reactions introduced in Table 1, which are based on the well known Zeldovich mechanism are taken into account.

Table 1. NOx formation reactions

	Stoichio metry	Rate: $k_i = k_{0,i}.T^{\alpha}.e^{\left(\frac{-TA_i}{T}\right)}$
R_1	$N_2 + O = NO + N$	$R_1 = k_1.CN_2.CO$
R_2	$O_2 + N = NO + O$	$R_2 = k_2.CO_2.CN$
R_3	$N + OH = NO + H$	$R_3 = k_3.COH.CN$
R_4	$N_2O + O = NO + NO$	$R_4 = k_4.CN_2O.CO$
R_5	$O_2 + N_2 = N_2O + O$	$R_5 = k_5.CO_2.CN_2$
R_6	$OH + N_2 = N_2O + H$	$R_6 = k_6.COH.CN_2$

All reactions rates r_i have units [mole/cm^{3}s] the concentrations c_i are molar concentrations under equilibrium conditions with units [mole/cm^3]. The concentration of N_2O is calculated according to:

$$\frac{N_2O}{N_2\sqrt{O_2}} = 1.1802.10^{-6}.T_1^{-0.6125}.exp\left[\frac{-18.71}{RT}\right] \quad (6)$$

NO formation rate is calculated as follows:

$$\frac{d[NO]}{dt} = 2(1-\alpha^2)\left[\frac{R_{1e}}{1+\alpha K_2} + \frac{R_{4e}}{1+K_4}\right]\frac{p}{RT} \quad (7)$$

The final rate of NO production/destruction in [mole/cm^{3}s] is calculated as:

$$r_{NO} = C_{PostProMult}.C_{kineticMult}.2(1-\alpha_2)\frac{r_1}{1+\alpha.AK_2}\frac{r_4}{1+AK_4} \quad (8)$$

with:

$$\alpha = \frac{C_{NO,act}}{C_{NO,equ}}.\frac{1}{C_{PostProMult}}$$

$$AK_2 = \frac{r_1}{r_2 + r_3}$$

$$AK_4 = \frac{r_4}{r_5 + r_6}$$

2.3.2. CO formation model

CO formation following two reactions given in Table 2 are taken into account:

Table 2: CO formation reactions

	Stoichio metry	Rate:
1	$CO + OH = CO_2 + H$	$r_1 = 6.76.10^{10}.e^{\left(\frac{T}{1102}\right)}.c_{CO}.c_{OH}$
2	$CO_2 + O = CO + O_2$	$r_2 = 2.51.10^{12}.e^{\left(\frac{-24055}{T}\right)}.c_{CO}.c_{O_2}$

The final rate of CO production/destruction in [mole/cm^{3}s] is calculated as:

$$r_{CO} = C_{const}.(r_1 + r_2).(1-\alpha) \quad (9)$$

with:

$$\alpha = \frac{c_{CO,act}}{c_{CO,equ}}$$

2.3.3. Soot formation model

Soot formation is described by two steps including formation and oxidation. The net rate of change in soot mass m_s is the difference between the rates of soot formed *ms.f* and oxidized $m_{s.ox}$.

$$\frac{dm_s}{dt} = \frac{dm_{s,f}}{dt} - \frac{dm_{s,ox}}{dt} \quad (10)$$

with:

$$\frac{dm_{s,f}}{dt} = A_f.m_{f,v}.p^{0,5}exp\left[\frac{-E_{s,f}}{RT}\right]$$

$$\frac{dm_{s,ox}}{dt} = A_{ox}.m_s\frac{P_{O2}}{P}.p^{1,8}exp\left[\frac{-E_{s,ox}}{RT}\right]$$

m_s: soot mass

$m_{f,v}$: fuel evaporation volume

P_{O2}: Pressure of O_2 molecules

$E_{s,f}$ = 52,335 kJ/kmol: activation energy

$E_{s,ox}$ = 58,615 kJ/kmol: oxidation energy

A_f, A_{ox}: the constant empiric selection and specific engine types.

2.4. Fuel Model

First, it is necessary to define fuel B100, B100 fuel is fuel 100% pure biodiesel including the chemical compound with the ratio by volume, and is presented in Table 3.

B10, B20, B30, B40 and B50 have a percentage of volume, respectively 10%, 20%, 30%, 40% and 50% of B100.

Table 3. Chemical composition of fuel B100

Chemical compound	Ratio (% volume)
$C_{15}H_{30}O_2$	0,0107
$C_{17}H_{34}O_2$	0,146
$C_{19}H_{38}O_2$	0,0655
$C_{19}H_{36}O_2$	0,399
$C_{19}H_{34}O_2$	0,376
$C_{19}H_{32}O_2$	0,0028

When defining the type of fuel (B0, B10, B20, B30, B40, and B50) to enter into the model, it is necessary to rely on the chemical formula and the ratio of each component. It's in the mix. In the case where diesel fuel (B0) has already been defined in the simulation software AVL-Boost, the remaining fuels must be entered with data based on the chemical model. Some of the main chemical and physical properties of the fuels are presented in Table 4.

Table 4. Some physical and chemical properties of the 6 fuels.

Properties	Unit	Method	B0	B10	B20	B30	B40	B50
Heating value	MJ/kg	ASTM D240	42.76	42.26	41.84	41.29	41.03	41.29
Cetane value		ASTM D613	49	50	51	52	53	54
Density at 15 ^oC	kg/m^3	ASTM D1298	838	840	845	848	852	857
Kinematic viscosity at 40 ^oC		ASTM D445	3.22	3.31	3.47	3.56	3.67	3.76
Flash point	cSt	ASTM D93	67	71	75	80	84	89
Sulfur content	ppm	ASTM D5453	428	430	433	436	439	441
Water content	ppm	ASTM D6304	62	84	96	110	122	136

2.5. Simulation Mode

The simulation mode will be performed in turn as follows: the amount of fuel supplied to the cycle will be fixed for all test fuels (B0, B10, B20, B30, B40, and B50). The amount of fuel supplied to the cycle according to the working modes for each load is presented in Table 5.

Table 5. The amount of fuel supplied to the cycle corresponding to the load values

Speed	Amount of fuel supplied to the cycle, g_{ct} (g)		
	75% load	50% load	25% load
1400 (rev/min)	0.0173	0.0115	0.00675

Step 1: Enter the corresponding input parameters when the engine is operating at 1400 rev/min with the early injection angle of 14 degrees, keeping the injection pressure at 600 psi (bar).

Step 2: Select the fuel model (B0, B10, B20, B30, B40, or B50). For each fuel, change gct to 25%, 50%, and 75% loads, respectively.

Step 3: Run the computational model and record the results of the combustion process, power, fuel consumption, and emissions.

2.6. Modeling Diesel Engine AVL 5402

The AVL 5402 engine is a single-cylinder, four-stroke, common rail diesel engine. The engine specification is shown in Table 6. The engine is modeled by AVL Boost software (Fig. 1).

Table 6. Specifications of the engine

N°	Parameter	Value
1	Cylinder diameter (D)	85 mm
2	Stroke (S)	90 mm
3	Displacement volume	510.7 cm^3
4	Compression ratio	17 : 1
5	Rate power/speed	9/3200 kW/rpm

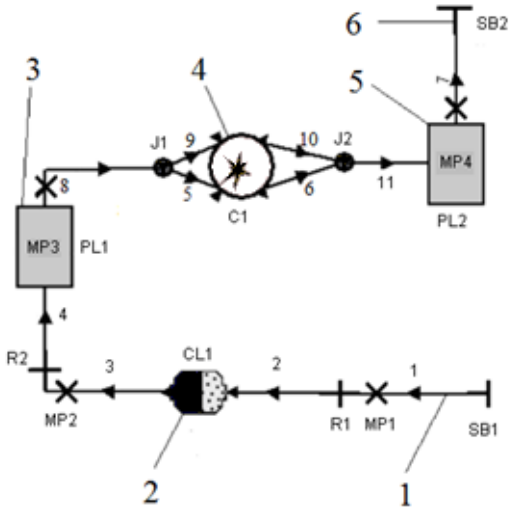

Fig. 1. Diesel engine AVL 5402 model

3. Results and Discussion

3.1. Model Validation

In order to determine the reliability of the calculation model before applying it on a large scale, it was necessary to use the model to calculate in a certain mode, compare the simulation results with the experimental measurement results, and adjust the measurement model if necessary so that the difference between the calculated results and measurement results is within the allowable limits.

Fig. 2 presents the results of comparisons of power (Fig 2a) and fuel consumption (Fig 2b) between simulation and experimental fuels B0, B10, B20, and B30 to keep the fuel supply corresponding to 75% load.

Results showed that the power and the fuel consumption between simulation and experiment matched quite well: the difference in power and fuel consumption was about 3.7% and 2.3%, respectively. Thus, it is possible to use this model to simulate the engine with biodiesel fuel.

3.2. Combustion Characteristics

Fig. 3 compares the pressure in the engine cylinder when using six kinds of fuel: B0, B10, B20, B30, B40, and B50. The results show that with an increasing proportion of blended biodiesel, the time of increasing pressure corresponds to the time of rapid fire, which means the speed of increasing pressure was decreased. Specifically, the time when the pressure separates from the compression line is understood as igniting. When the peak occurs earliest, the time of ignition and peak is gradually increased when the mixing ratio decreases and is maximum value for B0. The biodiesel fuel has a higher cetane rating value, which helps mix catch fire easily, resulting in the fire starting time being earlier. On the other hand, the peak pressure in the cylinder of B50 fuel is the lowest and increases gradually as the mixing ratio decreases. This can be explained by that the biodiesel-blend fuel mixture burns earlier and has a lower calorific value, leading to an increase in pressure during the fast combustion phase taking place in the limited compression stroke.

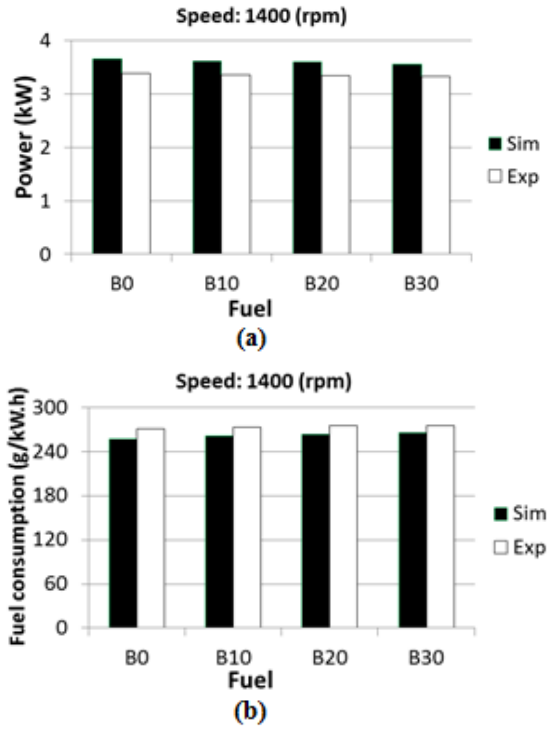

Fig. 2. Comparisons between simulation results and experiments

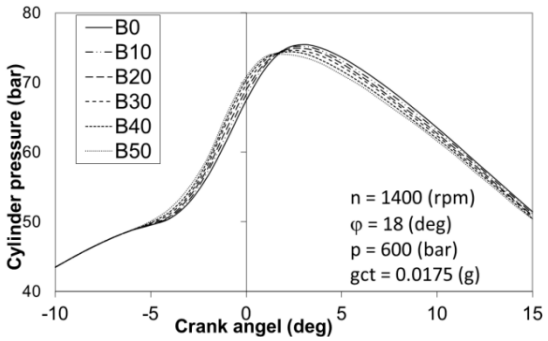

Fig. 3. Evolution of cylinder pressure of fuel B0, B10, B20, B30, B40 and B50.

Table 7. Comparison of combustion process parameters of 6 fuel types.

Combustion parameters	B0	B10	B20	B30	B40	B50
Cylinder pressure max (MPa)	75.46	75.25	74.91	74.52	74.31	74.08
Pressure angle max after TDC (^{0}TK)	3.29	3.02	2.80	2.67	2.23	2.01
Speed of increasing pressure max (MPa/^{0}TK)	5.68	5.67	5.60	5.58	5.53	5.48
Combustion starting angle before TDC (^{0}TK)	5.20	5.28	5.35	5.48	5.50	5.58
Calorific speeding max (J/^{0}TK)	167.5	165.1	163.2	159.6	157.5	156.3
Calorific angle max before TDC (^{0}TK)	0.5	0.6	0.7	0.85	1.0	1.1
Combustion parameters	75.46	75.25	74.91	74.52	74.31	74.08

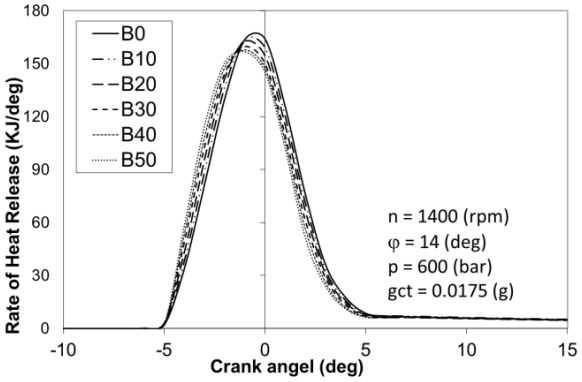

Fig. 4. Calorific speeding of types of fuel

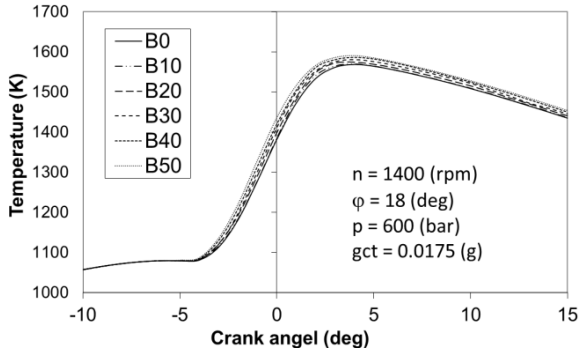

Fig. 5. Evolution of cylinder temperature of fuel B0, B10, B20, B30, B40 and B50

Specific parameters of combustion process are shown in Table 7.

The evolution of calorific speeding is shown in Fig. 4. The amount of fuel supplied to a cycle is the same for all fuels, except that the thermal power of biological fuel is lower than diesel fuel, so the calorific speed of biological diesel fuel is lower.

The rise time of calorific speed for biodiesel fuel will be earlier. It was explained by that the cetane rating value of biodiesel fuel is higher.

The temperature evolution in the cylinder is shown in Fig. 5. The results show that the temperature behavior of the fuels is similar. However, at each crank shaft position when starting to burn, the temperature in the cylinder of B50 fuel was the highest and gradually decreased as the biodiesel blending ratio decreased. On the other hand, the temperature value of fuel B0 is the smallest. This can be explained because biodiesel fuel has a higher cetane number, which makes the mixture easy to ignite. Moreover, when the mixture ignites in combination with the oxygen component available in the fuel, it helps the fuel oxidation process better. As a result, the combustion gas temperature is higher.

3.3. Engine Performance

The power of the engine is lower than using diesel fuel (B0) and decreases when the mix rate of biodiesel increases. With the respective fuels B10, B20, B30, B40, and B50, the average power loss in different load decreases was: 1,06%, 1,81%, 2,74%, 3,81%, and 4,79%. Amount of fuel supplied to a cycle is the same for all fuels, so power is reduced because the thermal value of biodiesel fuel is lower. The results also reduce power.

The fuel consumption rate increases with the increase of biodiesel fuel mix rate. With the respective fuels B10, B20, B30, B40, and B50, the average increasing rate was: 1,32%; 2,02%; 2,98%; 4,08%; and 5,55%. Because the amount of fuel supply is constant for fuel so the increase of biodiesel rate leads to reduce engine power.

The trend of power change and fuel consumption rate is shown in Fig. 6 and 7.

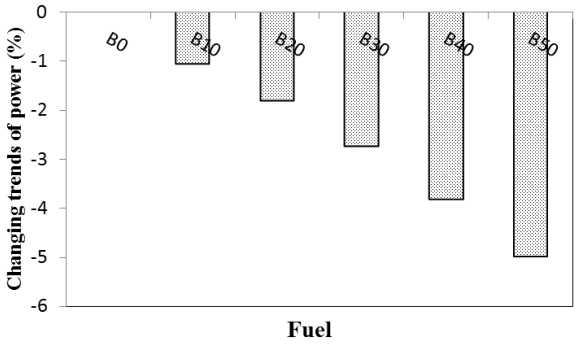

Fig. 6. The trend of power change.

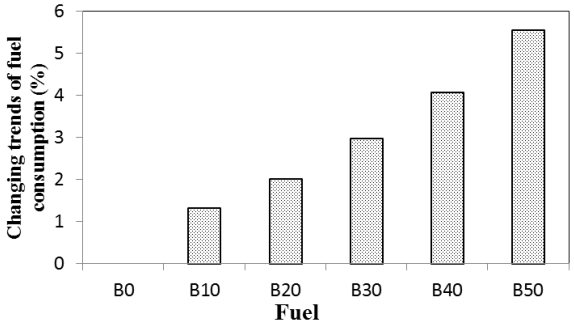

Fig. 7. The trend of fuel consumption rate change.

3.4. Air and Fuel Ratio A/F

When keeping the same fuel supply, the A/F ratio of the engine when using biodiesel fuel is always higher than that of conventional diesel fuel. This difference exists because the biodiesel fuel itself already has an O2 molecule. Meanwhile, with the same working mode of the engine, the amount of air entering the engine is the same for all fuels. The result is a larger A/F ratio (air residue factor) of the biodiesel fuel. The results of calculating the A/F ratio according to the simulation of the engine at different working modes for the investigated fuels are presented in Table 8.

3.5. Exhaust Emission

CO emissions are the product of combustion in a low-oxygen environment. When the engine uses biodiesel fuel, the biodiesel fuel has O_2 molecules, which leads to a reduction in the rich mixture area and, as a result, a decrease in CO emissions. CO emissions decreased while the biodiesel blend ratio increased. The results at different load modes are shown in Fig. 8. Accordingly, at 25% load, CO emissions decreased compared to B0 by 6.7%, 11.4%, 17.7%, 21.7%, 30.7%, respectively, at 50% load, 2.5%, 5.3%, 10.6, 16.6%, 21.6%, at 75% load, respectively, 4.9%, 9.2%, 13.7%, 18.4%, 26.8%, B10, B20, B30, B40, B50. On average, for different modes of load, the decrease in turn: 4.7%, 8.6%, 14.0%, 18.9%, 26.4%, with B10, B20, B30, B40, B50.

Table 8. Engine A/F ratio to fuels

Speed (rev/ min)	g_{ct} (g)	Fuel					
		B0	B10	B20	B30	B40	B50
1400	0.00675	75.29	75.43	75.58	75.64	75.79	75.95
	0.0115	44.17	44.32	44.47	44.62	44.77	44.92
	0.0173	29.86	30.14	30.44	30.74	31.03	31.33

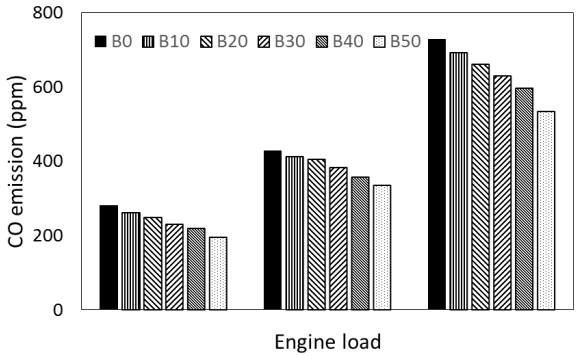

Fig. 8. CO emissions for fuel B0, B10, B20, B30, B40, B50

The conditions for NOx formation are the ratio of oxygen participating in the reaction and the reaction temperature. When we increase the ratio of biodiesel mixture to the corresponding emissions, NOx also increases. This change is due to the higher air/fuel ratio of biodiesel fuel, which creates favorable conditions for NOx formation. On the other hand, according to the results of the temperature in the cylinder as shown in Fig. 5, the temperature in the cylinder when using biodiesel fuel is higher than when using conventional diesel fuel. The higher the temperature, the higher the mixing ratio, this also explains why there is more NOx formation when using biodiesel fuel than when using conventional diesel fuel. The results are shown in Fig. 9 at 25%, 50%, and 75% load modes. Average for all load modes, NOx increased by 2.3%, 3.8%, 5.4%, 8.1%, and 10.5%, with B10, B20, B30, B40, and B50.

Results for soot of fuels at 25%, 50%, and 75% load modes are shown in Fig. 10.

Soot is a special pollutant in diesel engine exhaust. Diffusion combustion in diesel engines is very favorable for the formation of soot. However, with engines using biodiesel fuel, it has reduced emissions of soot because the fuel has oxygen elements that enable the soot oxidation process more thoroughly. Results showed that average soot for regimes loads was reduced by: 6,30%; 12,17%; 18,60%; 24,13%; and 30,03%, with B10, B20, B30, B40, and B50.

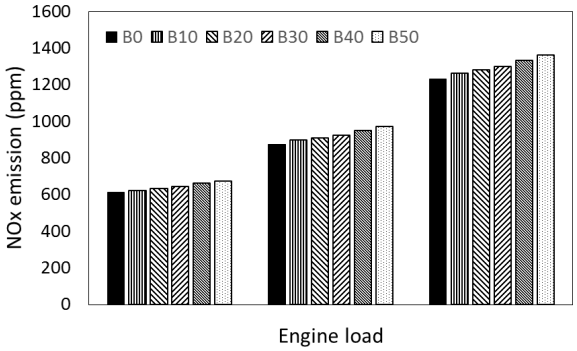

Fig. 9. NOx emissions for fuel B0, B10, B20, B30, B40, B50

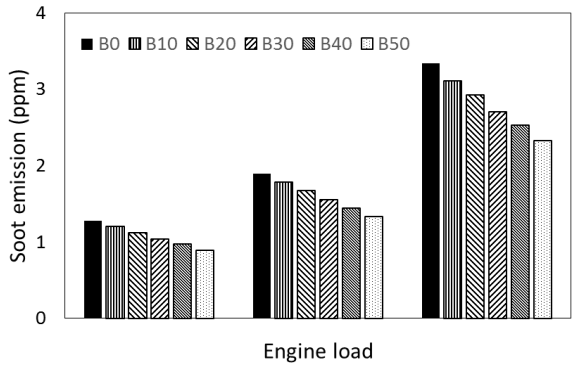

Fig. 10. Soot emissions for fuel B0, B10, B20, B30, B40, B50

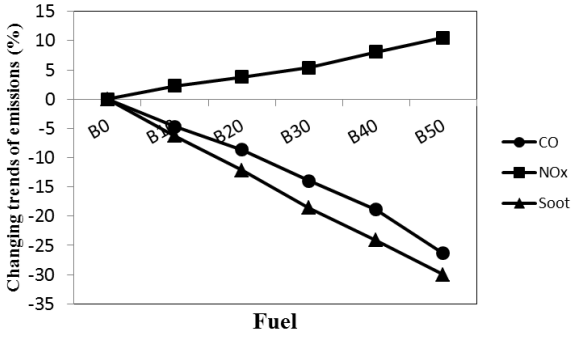

Fig. 11. Changing trends in engine emissions.

Changing trends of the toxic emissions of the engine when using B10, B20, B30, B40, and B50 compared to B0 is shown in Fig. 11.

As the biodiesel blending ratio increased, CO and soot emissions decreased while NOx increased. The rate of increase of NOx is obviously slower than that of CO and soot. Biodiesel fuel has a higher cetane number and has more oxygen in the fuel, which helps the combustion process take place and thus raises the combustion temperature. The high combustion temperature helps to oxidize the soot better, reducing the amount of soot but also creating favorable conditions for the formation of NOx.

4. Conclusion

The time of starting a fire is earlier when we increase the mixed biodiesel rate. Since biodiesel fuel has a higher cetane rating, the mixture will ignite better. Cylinder peak pressure trends to come first, but the value decreases with increasing biodiesel blending ratio. This occurs because biodiesel burns faster, but due to its lower calorific value, the peak pressure is also lower.

The temperature in the cylinder increases gradually as the biodiesel mixing ratio increases. The reason is that biodiesel fuel already has an oxygen component, which helps the combustion process to be more thorough, causing the combustion chamber temperature to increase.

The power of the engine tends to decrease while fuel consumption increases when using biodiesel. Accordingly, the largest reduction in power is 4.79% and the largest increase in fuel consumption is 5.55% for B50 fuel. However, due to the reduced combustion delay, both the combustion and compression processes occur at the same time.

CO emissions and soot levels are reduced, while NOx levels rise due to the mixed biodiesel rate.oxygen ingredients, the mixture fires better.

The trend of changing engine performance and emissions is positively dependent on the trend of changing biodiesel blending ratio.

References

[1] Graboski, M.S., McCormick, R.L., Combustion of fat and vegetable oil derived fuels in diesel engines. Prog. Energy Combust. Sci. 1998, 24, 125–164. https://doi.org/10.1016/S0360-1285(97)00034-8

[2] Shah, A.N., Yunshan, G., Chao, H., Combustion and emission response by a heavy-duty diesel engine fuelled with biodiesel: an experimental study, MUET. Available online: https://journal.uet.edu.pk/ojs_old/index.php/pjeas/article/view/243 (accessed on 20 May 2021).

[3] Nguyen Tuan Nghia, Le Anh Tuan, Tran Dang Quoc, A study on the effects of biodiesel blends based cat-fish fat on characteristics of a single cylinder diesel engine – AVL 5402, Journal of Transport Science and Technology, Special Issue, 7+8+9/2013. 47-51.

[4] Jinlin Xuea, Tony E. Grifta, Alan C. Hansena, Effect of biodiesel on engine performances and emissions, Renewable and Sustainable Energy Reviews 15 (2011) 1098–1116. https://doi.org/10.1016/j.rser.2010.11.016

[5] Lin B-F, Huang J-H, Huang D-Y, Experimental study of the effects of vegetable oil methyl ester on DI diesel engine performance characteristics and pollutant emissions, Fuel 2009, 88:1779–85. https://doi.org/10.1016/j.fuel.2009.04.006

[6] Ekrem Buyukkaya, Effects of biodiesel on a DI diesel engine performance, emission and combustion

characteristics, Contents lists available at ScienceDirect, 2010. https://doi.org/10.1016/j.fuel.2010.05.034

[7] Users Guide-AVL Boost Version 2011.1. Available online: https://www.avl.com/boost (accessed on 20 May 2021)

[8] Theory-AVL Boost Version 2011.1. Available online: https://www.avl.com/boost (accessed on 20 May 2021)

[9] G.Woschni , A universally applicable equation for the instantaneous heat transfer coefficient in internal combustion engines, SAE paper No. 6700931. (1967). https://doi.org/10.4271/670931

[10] Jiaqiang, E., Minh-Hieu, P., Yuanwang, D., Tuannghia, N., Vinh-Nguyen, D., Duc-Hieu, L., Wei, Z., Qingguo, P., Zhiqing, Z., Effects of injection timing and injection pressure on performance and exhaust emissions of a common rail diesel engine fueled by various concentrations of fish-oil biodiesel blends. Energy 2018, 149, 979–989. https://doi.org/10.1016/j.energy.2018.02.053

[11] Zhang, Z.E.J., Deng, Y., Pham, M., Zuo, W., Peng, Q., Yin, Z., Effects of fatty acid methyl esters proportion on combustion and emission characteristics of a biodiesel fueled marine diesel engine, Energy Convers. Manag., 2018, 159, 244–253. https://doi.org/10.1016/j.enconman.2017.12.098

[12] Nguyen, T.N., Pham, P.M., Tuan, L.A., Spray, combustion, performance and emission characteristics of a common rail diesel engine fueled by fish-oil biodiesel blends, Fuel 2020, 269, 117108. https://doi.org/10.1016/j.fuel.2020.117108